DIRECTIONAL COUPLER WITH GOOD RESTRAINT OUTSIDE THE PASSBAND AND ITS FREQUENCY-AGILE APPLICATION

Yujian Cheng[*], Lei Wang, Jie Wu, and Yong Fan

Fundamental Science on Extreme High Frequency Laboratory, School of Electronic Engineering, University of Electronic Science and Technology of China, Chengdu 611731, P. R. China

Abstract—In this paper, a directional coupler incorporating the bandpass frequency response characteristic is proposed and characterized. This structure is modified from a conventional branch-line coupler. Two wide open-ended coupled lines are used instead of microstrip branch lines. As such, good restraint performance outside the passband can be achieved. The even-odd mode technique is employed to analyze and synthesize such a coupler. After that, frequency tuning is achieved by modifying the electrical length of the open-ended coupled lines with varactors. Measured results validate the correctness of our theory and design.

1. INTRODUCTION

Directional couplers and filters are the most commonly used building blocks in microwave and RF systems. Considering the miniaturization design as one of the primary trends for transceivers, a single device integrated with different functionalities, such as filter-coupler [1–6], has been attracting increasing attention. It also recommends an effective way to avoid the performance degradation due to a cascade connection of two individual components. On the other hand, a number of reconfigurable microwave components, including frequency-agile couplers, have received significant attention because of their selectable fundamental characteristics [7–12]. Therefore, we hope to propose and design a 90-degree frequency-agile directional coupler incorporating with the filter's selectivity at each operation frequency
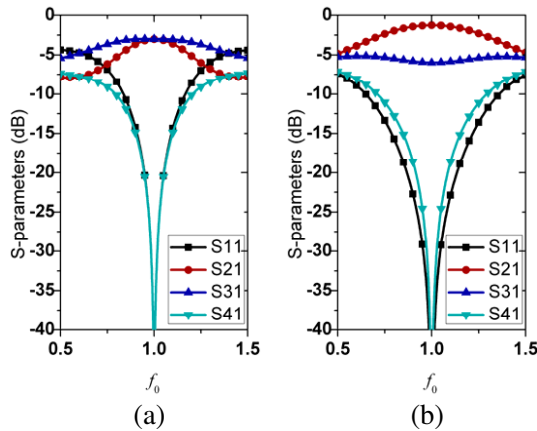
Figure 1. Calculated results of the conventional branch line directional coupler. (a) 3 dB coupling; (b) 6 dB coupling.

band. It is expected to yield better interference suppression compared with conventional frequency-agile coupler counterparts.

A branch-line coupler is a four-port network device with a 90° phase difference between two coupled ports. It consists of two microstrip lines linked by two transverse $\lambda/4$ branches located at $\lambda/4$ distance one from each other. As shown in Fig. 1, the conventional branch-line coupler usually has narrow bandwidth. However, its out of band characteristic has insufficient selectivity for adequate performance as a filter.

To achieve a directional coupler with good restraint outside the passband, two wide coupled open-circuited lines are employed instead of two microstrip line branches. Similar configurations can be found in [13, 14], but all of them are not appropriate for this design. Firstly, the coupled line has over-tight coupling when the design requirements are fulfilled. In this case, it is difficult to achieve the bandpass frequency response characteristic owing to the coupled line's wide passband. Secondly, all of these previous designs employ the shorted-ended lines, which are difficult to add varactors and achieve the electrical tunability. Section 2 introduces the theory analysis and design process in detail. The frequency electrically tunable method is proposed in Section 3. At last, a prototype is fabricated. It can operate within different frequency bands with different DC voltage bias.

2. DIRECTIONAL COUPLER BASED ON THE COUPLED TRANSMISSION LINE

2.1. Theory

Figure 2 illustrates the schematic of the proposed directional coupler. It consists of two microstrip branches and two open-ended coupled lines. As is well known, the coupled line is a widespread realization of microwave filters and has inherent bandpass frequency response characteristic. As such, a coupler including the coupled lines has the possibility to obtain good rejection out of the passband.

Here, the even-odd mode technique is employed to analyze such a model and synthesize the circuit. As shown in Fig. 3, two sub-networks are obtained by considering the open circuit for the even mode case and the short circuit for the odd mode case.

When $\theta_2 = \pi/2$, we readily obtain from these equivalent circuits:

$$[A]_e = \begin{bmatrix} 1 & 0 \\ jy & 1 \end{bmatrix} \begin{bmatrix} \frac{K_{11}}{K_{12}\tan(\theta_1)} & j\left(K_{12} - \frac{K_{11}^2}{K_{12}\tan^2(\theta_1)}\right) \\ \frac{j}{K_{12}} & \frac{K_{11}}{K_{12}\tan(\theta_1)} \end{bmatrix} \begin{bmatrix} 1 & 0 \\ jy & 1 \end{bmatrix} \tag{1}$$
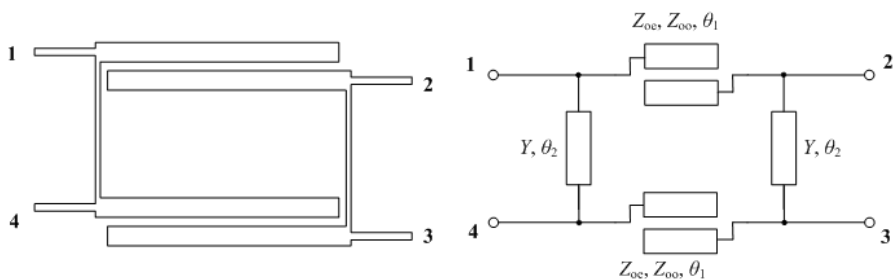

Figure 2. Configuration and equivalent schematic of the proposed coupler.
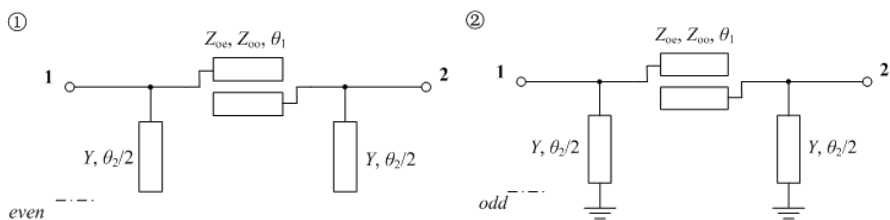

Figure 3. Even/odd models for the proposed directional coupler.

$$[A]_o = \begin{bmatrix} 1 & 0 \\ -jy & 1 \end{bmatrix} \begin{bmatrix} \frac{K_{11}}{K_{12}\tan(\theta_1)} & j\left(K_{12} - \frac{K_{11}^2}{K_{12}\tan^2(\theta_1)}\right) \\ \frac{j}{K_{12}} & \frac{K_{11}}{K_{12}\tan(\theta_1)} \end{bmatrix} \begin{bmatrix} 1 & 0 \\ -jy & 1 \end{bmatrix} \quad (2)$$

In (1), (2),

$$K_{11} = \frac{Z_{oe} + Z_{oo}}{2Z_0}, \quad K_{12} = \frac{Z_{oe} - Z_{oo}}{2Z_0} \quad (3)$$

Considering $\theta_1 = \pi/2$, S-parameters at the resonant frequency can be derived as follows:

$$S_{11} = \frac{1}{2}\left[\frac{j\left(1 - K_{12}^2 + y^2\right)}{-2y + j\left(1 + K_{12}^2 - y^2\right)} + \frac{j\left(1 - K_{12}^2 + y^2\right)}{2y + j\left(1 + K_{12}^2 - y^2\right)} \right]$$

$$S_{21} = \frac{1}{2}\left[\frac{2K_{12}}{-2y + j\left(1 + K_{12}^2 - y^2\right)} + \frac{2K_{12}}{2y + j\left(1 + K_{12}^2 - y^2\right)} \right]$$

$$S_{31} = \frac{1}{2}\left[\frac{2K_{12}}{-2y + j\left(1 + K_{12}^2 - y^2\right)} - \frac{2K_{12}}{2y + j\left(1 + K_{12}^2 - y^2\right)} \right] \quad (4)$$

$$S_{41} = \frac{1}{2}\left[\frac{j\left(1 - K_{12}^2 + y^2\right)}{-2y + j\left(1 + K_{12}^2 - y^2\right)} - \frac{j\left(1 - K_{12}^2 + y^2\right)}{2y + j\left(1 + K_{12}^2 - y^2\right)} \right]$$

If

$$S_{11} = 0, \quad S_{21} = 0 \quad (5)$$

There is

$$1 + K_{12}^2 = y^2 \quad (6)$$

And then

$$S_{31} = \frac{-K_{12}}{y}, \quad S_{41} = \frac{-j}{y} \quad (7)$$

2.2. Calculation Examples

Based on the above proposed configuration, (7) can be used to design a coupler with arbitrary coupling level. For example, considering

$$|S_{31}| = |S_{41}| \quad (8)$$

That is a 3 dB coupling case. Here,

$$K_{12} = 1, \quad y = \sqrt{2} \quad (9)$$

That means,

$$Z_{oe} - Z_{oo} = 100 \quad (10)$$
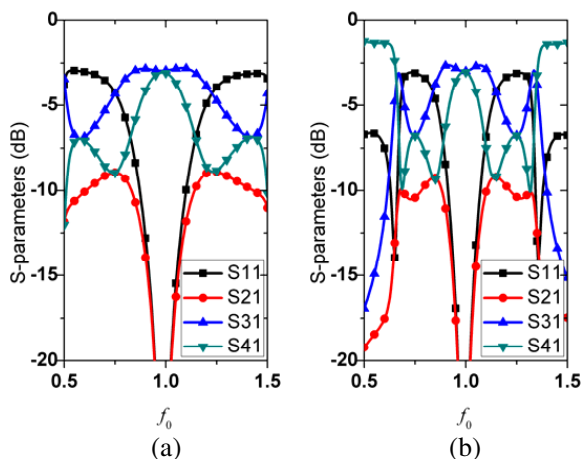
$$Y = 1/35.35 \quad (11)$$

Figure 4. Calculated results of the proposed directional coupler. (a) $Z_{oe}/Z_{oo} = 130/30$; (b) $Z_{oe}/Z_{oo} = 180/80$.

Now, the S-parameters of the ideal model (as shown in Fig. 2) versus different Z_{oe}/Z_{oo} values are calculated and depicted in Fig. 4. It is demonstrated that the bandwidth of this coupler can be controlled by Z_{oe}/Z_{oo}. But the out-of-passband suppression is not apparent and it still cannot effectively filter out-of-band signals. That is because (10) generally leads to a strong coupling for a coupled line. The coupled line with the strong coupling has a wide passband (Fig. 5 presents the calculated frequency response characteristics of the coupled lines). It is known that the branch-line coupler usually has narrow bandwidth. By use of a coupled line with wide passband, the coupler's frequency selectivity can be improved but the extent is limited.

As shown in Figs. 4, 5, it is expected that higher Z_{oe} and Z_{oo} can narrow the coupled line's bandwidth and then narrow the coupler's bandwidth. However, it is unfeasible in normal printed circuit board (PCB) fabrication due to the constraint on narrow line width and small gap dimensions.

To solve this weakness, the coupled line is widened to reduce its coupling ratio. The passband can be narrowed through normal PCB fabrication process, which overcomes the realization difficulties. Here, the wide line width out of range leads to the inaccuracy of those existed design formula for a coupled-line pair. The foregoing analysis is no longer applicable because there is no accurate analytic expression for the coupled line's ABCD transfer matrix. As such, another equivalent model is proposed in Fig. 6. Two open-ended coupled lines are considered as two "black boxes" with the function of bandpass filters.
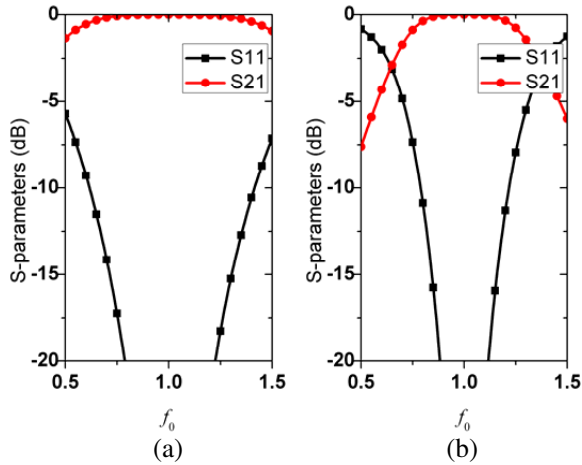
Figure 5. Calculated results of the coupled line. (a) $Z_{oe}/Z_{oo} = 130/30$; (b) $Z_{oe}/Z_{oo} = 180/80$.
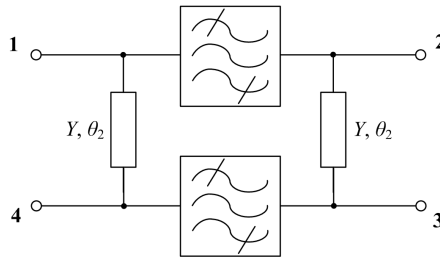

Figure 6. Another equivalent schematic of the proposed directional coupler.

Here, we don't pay attention to the coupled line's transfer matrix, but pay attention to its S-parameters. The coupler's frequency response characteristic, such as the suppression bandwidth, is directly determined by the black box's frequency selectivity. Besides, the coupler's coupling level can be achieved by optimizing dimensions of the coupled lines and microstrip lines. As an example, a 3 dB coupler is designed with different suppression bandwidths. Simulated results implemented by ADS are shown in Fig. 7. Their out-of-band suppression is much better compared with the above designs. The phase differences between output ports 3 and 4 are 90° at each center frequency of those cases. Fig. 8 shows S-parameters of the coupled lines with the same dimensions. It is demonstrated that the bandwidths of the coupler and the corresponding coupled line are almost the same.
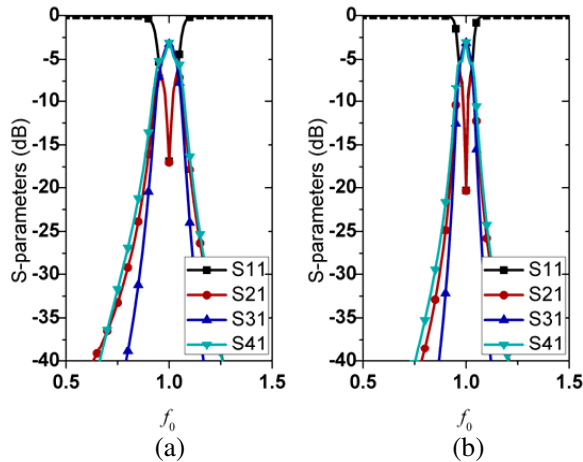
Figure 7. Simulated results of the proposed 3 dB directional coupler by use of wide coupled lines with different bandwidth. (a) The Coupled line width $w_c/\lambda = 0.1247$, the coupled line gap width $g_c/\lambda = 0.0006$, the coupled line length $l_c/\lambda = 0.5307$, the microstrip line width $w_m/\lambda = 0.0016$, the microstrip line length $l_m/\lambda = 0.0875$, and the substrate height $h = 0.0031$; (b) $w_c/\lambda = 0.2183$, $g_c/\lambda = 0.0025$, $l_c/\lambda = 0.58$, $w_m/\lambda = 0.0063$, $l_m/\lambda = 0.1559$, and $h = 0.0031$.

However, the center frequency of the coupled line is a little lower than that of the coupler. As another example, a 6 dB coupler is designed with different suppression bandwidth as shown in Fig. 9. The phase differences between output ports 3 and 4 are also 90° at each center frequency of those cases.

3. FREQUENCY-AGILE APPLICATION

After finishing the analysis and design of the static coupler incorporating the bandpass frequency response characteristic, the frequency-agile application is investigated in this section. The first task is to construct a frequency-agile coupled line. Here, each coupled line's end is connected with a varactor. As shown in Fig. 10, the change in capacitance will modify the electrical length of the coupled line, and then change the operation frequency.

Then, this frequency-agile coupled line is employed in the coupler design. For circuit feasible, the other end of the coupled line is extended to connect with the microstrip branches. As shown in Figs. 11 and 12, an L-band 6 dB frequency-agile bandpass coupler is designed and fabricated on the substrate Taconic RF35 with the relative permittivity
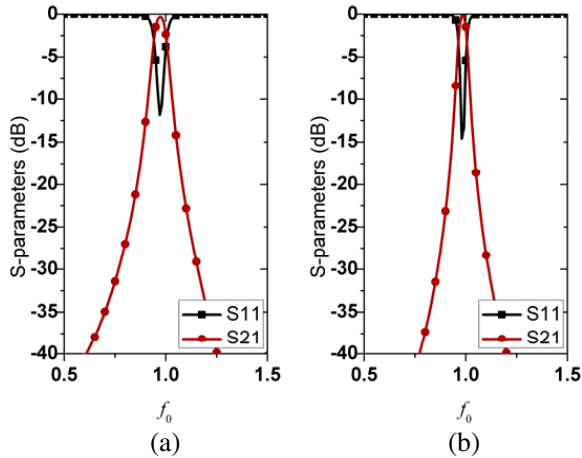
Figure 8. Simulated results of the wide coupled line corresponding to the 3 dB model in Figure 7. (a) $w_c/\lambda = 0.1247$, $g_c/\lambda = 0.0006$, $l_c/\lambda = 0.5307$, and $h = 0.0031$; (b) $w_c/\lambda = 0.2183$, $g_c/\lambda = 0.0025$, $l_c/\lambda = 0.58$, and $h = 0.0031$.
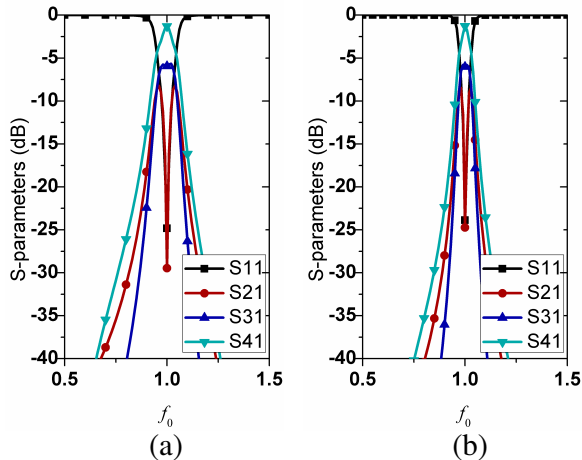

Figure 9. Simulated results of the proposed 6 dB directional coupler by use of wide coupled lines with different bandwidth. (a) $w_c/\lambda = 0.1185$, $g_c/\lambda = 0.0026$, $l_c/\lambda = 0.5294$, $w_m/\lambda = 0.0011$, $l_m/\lambda = 0.075$, and $h = 0.0031$; (b) $w_c/\lambda = 0.1996$, $g_c/\lambda = 0.0065$, $l_c/\lambda = 0.5145$, $w_m/\lambda = 0.0044$, $l_m/\lambda = 0.1434$, and $h = 0.0031$.

of 3.5 and the height of 0.508 mm. The used varactor is Skyworks SMV1405. The DC bias is applied to two ports via bias Tees, and DC blocking capacitors are placed at other ports.
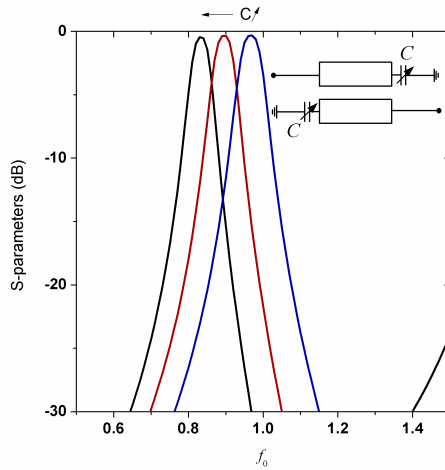
Figure 10. ADS simulated results of the proposed frequency-agile coupled line with $C_{\max}/C_{\min} = 20$, $w_c/\lambda = 0.1247$, $g_c/\lambda = 0.0006$, $l_c/\lambda = 0.5307$, and $h = 0.0031$.
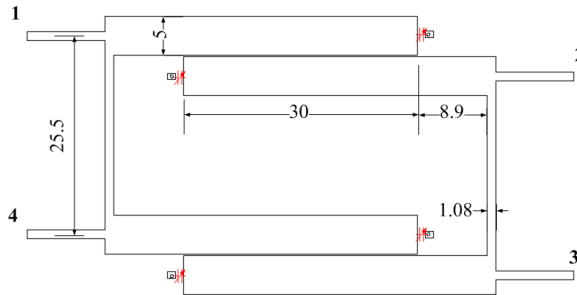

Figure 11. Configuration and dimension of the proposed directional coupler. (Units: mm, gap: 0.2 mm).
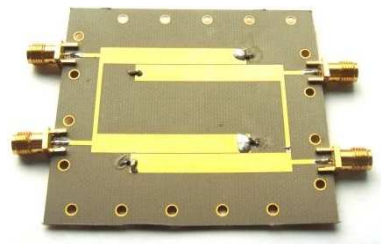

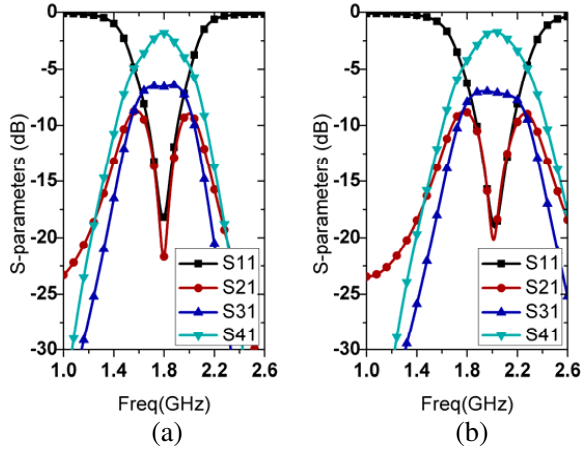**Figure 12.** Photograph of the fabricated directional coupler.

Figure 13. Simulated results of the fabricated directional coupler.
(a) $C = 2.67\,\mathrm{pF}$; (b) $C = 0.89\,\mathrm{pF}$.

Table 1. Bandpass filtering characteristics of the proposed coupler
with different bias voltages.

V_{bias} (V)	Frequency (GHz)	Suppression of S_{31} (dB)	Suppression of S_{41} (dB)
0	1.04	30	33
	1.23	20	19
	1.40	10	9
	2.03	10	8
	2.15	20	14
	2.24	30	20
	2.38	31	30
16.2	1.20	30	33
	1.44	20	18
	1.62	10	9
	2.42	10	8
	2.57	20	15
	2.82	30	28

The Ansoft HFSS simulated results of the optimized coupler
with different capacitances and the measured results of the fabricated
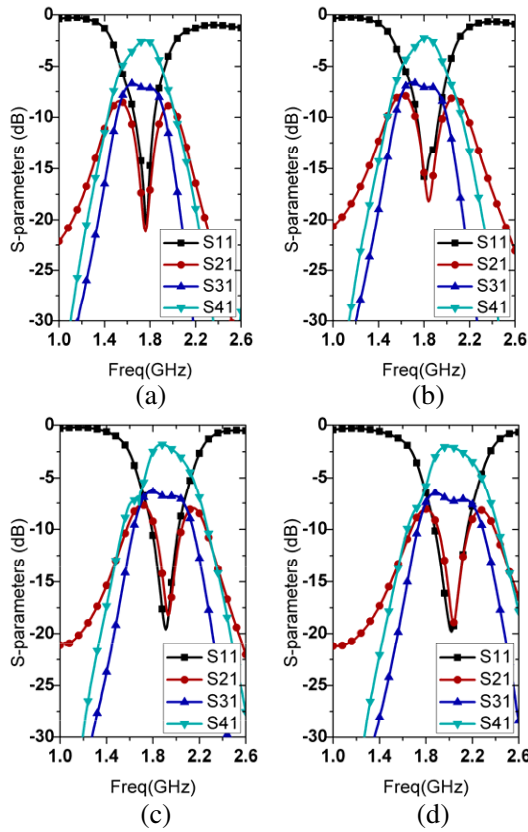coupler with different bias voltages are depicted in Figs. 13 and 14,

Figure 14. Measured results of the fabricated directional coupler. (a) $V_{bias} = 0$ V; (b) $V_{bias} = 0.7$ V; (c) $V_{bias} = 2.3$ V; (d) $V_{bias} = 16.2$ V.
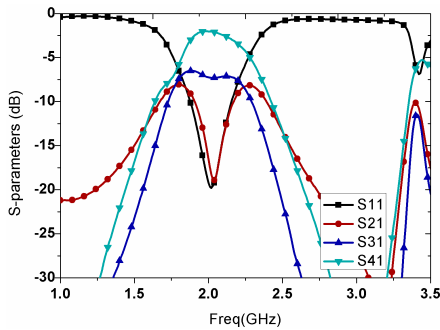

Figure 15. Measured results of the fabricated directional coupler with $V_{bias} = 16.2$ V to present the suppression characteristic.

respectively. When V_{bias} is varied from 0 to 16.2 V, the coupler's center frequency is varied from 1.81 to 2.07 GHz. At the center frequency of each operation mode, the return loss is better than 15 dB, the isolation is better than 18 dB, and the average insertion loss is about 1.2 dB. Table 1 exhibits the coupler's bandpass filtering characteristics with different bias voltages. As shown in Fig. 15, there exists parasitic passbands for the fabricated coupler considering the frequency response characteristic of the coupled-line. When $V_{bias} = 0$ V, the phase difference between ports 3 and 4 is $90° \pm 5°$ over $1.78 \sim 1.84$ GHz. When $V_{bias} = 16.2$ V, the phase difference between ports 3 and 4 is $90° \pm 5°$ over $2.02 \sim 2.12$ GHz.

4. CONCLUSION

A varactor tunable directional coupler with good out-of-passband rejection has been investigated and experimented. First, a static bandpass coupler with controllable coupling level and suppression bandwidth has been theoretically analyzed and designed. Then, a frequency-agile coupler has been realized by inserting varactors as loads of the open-ended coupled lines in order to control and modify the operation frequency. Satisfactory agreement between the measurements and analysis has been demonstrated.

ACKNOWLEDGMENT

REFERENCES

1. Uchida, H., N. Yoneda, Y. Konishi, and S. Makino, "Bandpass directional couplers with electromagnetically-coupled resonators," *IEEE MTT-S Int. Microw. Symp. Dig.*, 1563–1566, 2006.

2. Wang, W. H., T. M. Shen, T. Y. Huang, and R. B. Wu, "Miniaturized rat-race coupler with bandpass response and good stopband rejection," *IEEE MTT-S Int. Microw. Symp. Dig.*, 709–712, 2009.

3. Shen, T. M., T. Y. Huang, C. F. Chen, and R. B. Wu, "A laminated waveguide magic-T with bandpass filter response in multilayer LTCC," *IEEE Trans. on Microw. Theory and Tech.*, Vol. 59, No. 3, 584–592, Mar. 2011.

4. Wong, Y. S., S. Y. Zheng, and W. S. Chan, "Multifolded bandwidth banch line coupler with filtering characteristic using coupled port feeding," *Progress In Electromagnetics Research*, Vol. 118, 17–35, 2011.

5. Lin, C. K. and S. J. Chung, "A compact filtering 180° hybrid," *IEEE Trans. on Microw. Theory and Tech.*, Vol. 59, No. 12, 3030–3036, Dec. 2011.

6. Cheng, Y. J. and Y. Fan, "Compact substrate-integrated waveguide bandpass rat-race coupler and its microwave applications," *IET Microw. Antennas Propag.*, Vol. 6, No. 9, 1000–1006, Jul. 2012.

7. Djoumessi, E., E. Marsan, C. Caloz, M. Chaker, and K. Wu, "Varactor tuned dual-band quadrature hybrid coupler," *IEEE Microw. Wirel. Compon. Lett.*, Vol. 16, No. 11, 603–605, Nov. 2006.

8. Chen, J.-X., J. Shi, Z.-H. Bao, and Q. Xue, "Tunable and switchable bandpass filters using slot-line resonators," *Progress In Electromagnetics Research*, Vol. 111, 25–41, 2011.

9. Costa, F. and A. Monorchio, "Design of subwavelength tunable and steerable Fabry-Perot/leaky wave antennas," *Progress In Electromagnetics Research*, Vol. 111, 467–481, 2011.

10. Lee, W.-S., H.-L. Lee, K.-S. Oh, and J.-W. Yu, "Switchable distance-based impedance matching networks for a tunable HF system," *Progress In Electromagnetics Research*, Vol. 128, 19–34, 2012.

11. Martinez-Lopez, R., J. Rodriguez-Cuevas, A. E. Martynyuk, and J. I. Martinez Lopez, "An active ring slot with RF mems switchable radial stubs for reconfigurable frequency selective surface applications," *Progress In Electromagnetics Research*, Vol. 128, 419–440, 2012.

12. Cheng, Y. J., "Substrate integrated waveguide frequency-agile slot antenna and its multibeam application," *Progress In Electromagnetics Research*, Vol. 130, 153–168, 2012.

13. Gipprich, J. W., "A newclass of branch-line directional couplers," *IEEE MTT-S Int. Microw. Symp. Dig.*, 589–592, 1993.

14. Fathelbab, W. M., "The synthesis of a class of branch-line directional couplers," *IEEE Trans. on Microw. Theory and Tech.*, Vol. 56, No. 8, 1985–1994, Aug. 2008.